CONTENTS

NASA Technical Paper 1212

Microwave Emission From Polar Firn

A. T. C. Chang and B. J. Choudhury

APRIL 1978

NASA

NASA Technical Paper 1212

Microwave Emission From Polar Firn

A. T. C. Chang
Goddard Space Flight Center
Greenbelt, Maryland

B. J. Choudhury
Computer Sciences Corporation
Silver Spring, Maryland

National Aeronautics
and Space Administration

**Scientific and Technical
Information Office**

1978

MICROWAVE EMISSION FROM POLAR FIRN

A. T. C. Chang
Goddard Space Flight Center
Greenbelt, Maryland

B. J. Choudhury
Computer Sciences Corporation
Silver Spring, Maryland

INTRODUCTION

Brightness temperatures obtained from the Electrically Scanning Microwave Radiometer (ESMR) 1.55-cm wavelength experiment on board the Nimbus-5 spacecraft over Greenland and Antarctica (Reference 1) have shown a lack of correlation with the physical surface temperature. The model study of microwave emission from a half-space with scattering and absorbing centers by A. W. England and T. C. Chang et al. (References 2 and 3) calculated the brightness temperature for a model snow field consisting of randomly spaced ice spheres of different radii and dielectric properties. The scattering and extinction cross sections were calculated using the Mie-scattering theory and the brightness temperature values were then obtained by numerically solving the radiative transfer equation. Results of the calculation showed that the emerging microwave radiation originates deep within the medium. These results not only provided an explanation for the lack of correlation of the observed brightness temperatures and the physical surface temperatures but also opened up the possibility of remotely sensing such parameters as the snow accumulation rate and snow temperature profile.

In the model calculations performed by T. C. Chang et al. and A. W. England (References 3, 2 and 4), the scattering and absorption properties have been assumed to be independent of the snow depth. This is in contrast to the actual situation where the crystal size does vary with the snow depth (References 5 and 6). Also, in the former work the physical temperature of snow has been taken to be independent of depth and in the latter calculation a linear temperature variation has been used. The accuracy of the numerical results obtained by A. W. England (Reference 4) is difficult to assess because of the convergence problem associated with his method of solution (Reference 2). Here we have attempted to provide a quantitative explanation for the radio brightness temperature observed over Greenland and Antarctica by the ESMR on board the Nimbus-5 satellite. Scattering and absorption parameters used in the calculation are those compiled by H. J. Zwally (Reference 7) by fitting the crystal size data measured by A. J. Gow (References 5 and 6) at different snow depths. Seasonal and depth variation of temperature have also been taken into account. The radiative transfer equation, equation (1), has been solved numerically using these snow parameters

by the method of invariant imbedding by S. Chandrasekhar (Reference 8), R. E. Bellman et al. (Reference 9), R. Redheffer (Reference 10), R. W. Preisendorfer (Reference 11), and I. P. Grant and G. E. Hunt (Reference 12). The accuracy of the calculations has been verified by comparing the numerical results with those obtained by S. Chandrasekhar (Reference 8) for the law of darkening for the conservative case of perfect scattering with Rayleigh and isotropic scattering phase function in a semi-infinite plane parallel medium.

NUMERICAL SOLUTION FOR THE RADIATIVE TRANSFER EQUATION

The radiative transfer equation for an axially symmetric inhomogeneous medium in which all interactions are linear can be written in the form of an integro-differential equation (Reference 12)

$$\mu \frac{dI(x, \mu)}{dx} = -\sigma(x) I(x, \mu) + \sigma(x) \left\{ [1 - \omega(x)] B(x) + \frac{1}{2} \omega(x) \int_{-1}^{1} p(x, \mu, \mu') I(x, \mu') d\mu' \right\} \quad (1)$$

where the radiation intensity $I(x, \mu)$ is at depth x traveling in the direction making an angle whose cosine is μ with the normal toward the direction of increasing x (Figure 1).

The functions $\sigma(x)$, $\omega(x)$, $B(x)$, and $p(x, \mu, \mu')$ are prescribed functions of their arguments. They are referred to as the extinction per unit length, the single scattering albedo, the source, and the phase function, respectively. For a nonuniform medium these functions are generally piecewise continuous functions of depth subject to the conditions

$$B(x) \geq 0, \sigma(x) \geq 0, 0 \leq \omega(x) \leq 1, p(x, \mu, \mu') \geq 0. \quad (2)$$

In the present work, the following normalization for the phase function will be used

$$\frac{1}{2} \int_{-1}^{1} p(x, \mu, \mu') d\mu' = 1 \quad (3)$$

for all values of x.

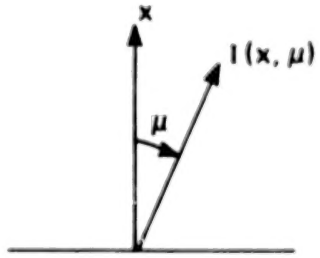

Figure 1. Radiation intensity of $I(x, \mu)$.

Instead of working with depth x, one generally works with a dimensionless depth variable called optical depth τ, defined in differential form as

$$d\tau = \sigma(x)\,dx. \tag{4}$$

In terms of optical depth, equation (1) reduces to

$$\mu \frac{dI(\tau, \mu)}{d\tau} = -I(\tau, \mu) + [1 - \omega(x)]\,B(x)$$

$$+ \frac{1}{2}\,\omega(\tau) \int_{-1}^{+1} p(\tau, \mu, \mu')\,d\mu\, I(\tau, \mu'). \tag{5}$$

The principle of invariance replaces the equation of transfer, equation (5), by an operator equation. This operator equation has the characteristic of mapping the fluxes incident on the boundaries of a medium from outside to the emergent fluxes. This mathematical mapping operator can be separated into two physical operators called reflectance and transmittance operators.

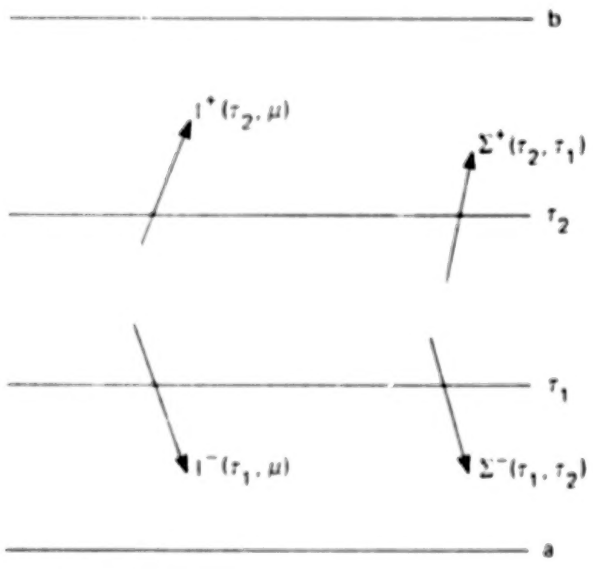

Figure 2. Source and incident intensity.

Consider an arbitrary layer bounded by planes with coordinates τ_1 and τ_2 within a medium which is bounded between the layers $\tau = a$ and $\tau = b$, i.e., $a \leq \tau_1 < \tau_2 \leq b$ (Figure 2). The intensities impinging on this layer are $I^+(\tau_1, \mu)$ and $I^-(\tau_2, \mu)$. The principle of invariance demands that the emergent intensities $I^+(\tau_2, \mu)$ and $I^-(\tau_1, \mu)$ will depend linearly on the incident intensities $I^+(\tau_1, \mu)$, $I^-(\tau_2, \mu)$ and on the intensities $\Sigma^-(\tau_1, \tau_2)$ and $\Sigma^+(\tau_2, \tau_1)$, which are generated by the sources within the layer. In other words, one can write

$$I^+(\tau_2, \mu) = t(\tau_2, \tau_1)\,I^+(\tau_1, \mu) + r(\tau_1, \tau_2)\,I^-(\tau_2, \mu) + \Sigma^+(\tau_2, \tau_1) \tag{6}$$

and

$$I^-(\tau_1, \mu) = t(\tau_1, \tau_2)\, I^-(\tau_2, \mu) + r(\tau_2, \tau_1)\, I^+(\tau_1, \mu) + \Sigma^-(\tau_1, \tau_2).$$

In matrix notation, equation (6) can be written as

$$\begin{bmatrix} I^+(\tau_2, \mu) \\ \\ I^-(\tau_1, \mu) \end{bmatrix} = S(\tau_1, \tau_2) \begin{bmatrix} I^+(\tau_1, \mu) \\ \\ I^-(\tau_2, \mu) \end{bmatrix} + \Sigma(\tau_1, \tau_2) \tag{7}$$

where the S-matrix is the exact mapping operator in the absence of internal sources

$$S(\tau_1, \tau_2) = \begin{bmatrix} t(\tau_2, \tau_1) & r(\tau_1, \tau_2) \\ \\ r(\tau_2, \tau_1) & t(\tau_1, \tau_2) \end{bmatrix}$$

and the $\Sigma(\tau_1, \tau_2)$ is the contribution of internal sources to the emergent intensities

$$\Sigma(\tau_1, \tau_2) = \begin{bmatrix} \Sigma^+(\tau_2, \tau_1) \\ \\ \Sigma^-(\tau_1, \tau_2) \end{bmatrix}$$

The response operators r and t defined through equation (6) are in general nonlocal integral operators. In physical terms these operators represent the transmission (t) and the reflection (r) characteristics of the layer bounded by the arguments of these operators. For a source-free medium, the knowledge of these operators is sufficient to predict all radiative transfer characteristics of that medium as one can expect from equation (7).

The radiative transfer equation (1) contains an integral over-the-angle variable. Numerically any integration requires a discrete variable representation. A quadrature representation will be imposed for this angular integration; the choice of quadrature will remain arbitrary. With this understanding, a set of values is selected for μ

$$\{\mu_j, \ 1 \leq j \leq m, \ 0 < \mu_j \leq 1\}. \tag{8}$$

With this set of values, the quadrature formula requires that weights C_j be associated such that for a function $f(\mu)$

$$\int_0^1 f(\mu)\, d\mu \approx \sum_{j=1}^{m} f(\mu_j)\, C_j. \tag{9}$$

Since the choice of equation (8) requires that all angle variables be positive, and examination of equation (6) shows that one set of radiation is going in the positive direction and the other is going in the negative direction, two vectors representing the propagation direction (positive and negative) of the radiation will be defined as:

$$\begin{aligned} u^+(x) &= \left\{ I(x, \mu);\ 0 \leq \mu \leq 1 \right\} \\ u^-(x) &= \left\{ I(x, -\mu);\ 0 \leq \mu \leq 1 \right\} \end{aligned} \tag{10}$$

Explicitly, the vector $u^+(x)$ is

$$u^+(x) = \begin{bmatrix} I(x, \mu_1) \\ I(x, \mu_2) \\ I(x, \mu_3) \\ \cdot \\ \cdot \\ \cdot \\ I(x, \mu_m) \end{bmatrix} \tag{11}$$

One can easily verify that the radiative transfer equation (1) can be written in terms of $u^+(x)$ and $u^-(x)$ as

$$M \frac{du^+(x)}{dx} + u^+(x) = [1 - \omega(x)]\, B(x) + \frac{1}{2}\omega(x) \left[p^{++}(x)\, C\, u^+(x) + p^{+-}(x)\, C\, u^-(x) \right] \tag{12}$$

$$-M \frac{du^-(x)}{dx} + u^-(x) = [1 - \omega(x)]\, B(x) + \frac{1}{2}\omega(x) \left[p^{-+}(x)\, C\, u^+(x) + p^{--}(x)\, C\, u^-(x) \right]$$

where M and C are m x m diagonal matrices of quadrature angles and weights

$$\mathbf{M} = |\mu_i \delta_{ij}| \qquad \mathbf{C} = |C_i \delta_{ij}|$$

and phase functions p^{++}, p^{+-}, p^{-+}, and p^{--} can be expressed as:

$$p^{++}(x) = \left\{ p(x, \mu_i, \mu_j) \right\}$$

$$p^{+-}(x) = \left\{ p(x, \mu_i, -\mu_j) \right\}$$

$$p^{-+}(x) = \left\{ p(x, -\mu_i, \mu_j) \right\}$$

$$p^{--}(x) = \left\{ p(x, -\mu_i, -\mu_j) \right\}$$

Note that in equation (12) if the internal source term B(x) has directional characteristics (i.e., it is a function of μ), one should also write these terms as vectors in the same way as the intensity vectors defined in equation (11). For the sake of simplicity of notation the following symbolic matrices and vectors constructed from equation (12) are defined:

$$\begin{aligned}
\Gamma^{++}(x) &= \mathbf{M}^{-1} \left[\mathbf{1} - \frac{1}{2} \omega(x)\, p^{++}(x)\, \mathbf{C} \right] \\
\Gamma^{+-}(x) &= \mathbf{M}^{-1} \left[\frac{1}{2} \omega(x)\, p^{+-}(x)\, \mathbf{C} \right] \\
\Gamma^{-+}(x) &= \mathbf{M}^{-1} \left[\frac{1}{2} \omega(x)\, p^{-+}(x)\, \mathbf{C} \right] \\
\Gamma^{--}(x) &= \mathbf{M}^{-1} \left[\mathbf{1} - \frac{1}{2} \omega(x)\, p^{--}(x)\, \mathbf{C} \right] \\
\Sigma^{+}(x) &= \mathbf{M}^{-1} \left[1 - \omega(x) \right] \mathbf{B}(x) \\
\Sigma^{-}(x) &= \mathbf{M}^{-1} \left[1 - \omega(x) \right] \mathbf{B}(x)
\end{aligned} \tag{13}$$

In equation (13), I denotes an m x m identity matrix; $\Gamma^{++}(x)$, $\Gamma^{+-}(x)$, $\Gamma^{-+}(x)$, and $\Gamma^{--}(x)$ are m x m matrices; and $\Sigma^{+}(x)$ and $\Sigma^{-}(x)$ are vectors of order m. In terms of these symbols, equation (12) can be written as:

$$\frac{du^+}{dx} = -\Gamma^{++}(x)\,u^+(x) + \Gamma^{+-}(x)\,u^-(x) + \Sigma^+(x)$$

$$-\frac{du^-}{dx} = \Gamma^{-+}(x)\,u^+(x) - \Gamma^{--}(x)\,u^-(x) + \Sigma^-(x). \qquad (14)$$

Equation (14) is the representation of the radiative transfer equation (1) within the quadrature approximation.

One can now consider an infinitesimal layer bounded between optical depths x and y ($y > x$) and a point ξ within this layer, i.e.,

$$x < \xi < y$$

A finite difference approximation to the lefthand side of equation (14) will be

$$\frac{du^+}{dx} \approx \frac{u^+(y) - u^+(x)}{(y - x)}$$

$$\frac{du^-}{dx} \approx \frac{u^-(y) - u^-(x)}{(y - x)} \qquad (15)$$

On the righthand side of equation (14), the intensity vectors u^+ and u^- will be evaluated at their boundary of incidence, i.e., at the optical depth x and y, respectively. This allows one to write equation (14) in the finite difference notation as:

$$\frac{u^+(y) - u^+(x)}{y - x} = -\Gamma^{++}(\xi)\,u^+(x) + \Gamma^{+-}(\xi)\,u^-(y) + \Sigma^+(\xi)$$

$$\frac{u^-(x) - u^-(y)}{y - x} = \Gamma^{-+}(\xi)\,u^+(x) - \Gamma^{++}(\xi)\,u^-(y) + \Sigma^-(\xi) \qquad (16)$$

Equation (16) now can be cast in the form given by equation (6). One can thus identify the reflection and the transmission operators of this infinitesimal layer as

$$
\begin{aligned}
t(y, x) &= I - \Gamma^{+\,+}(\xi)\,(y - x) \\
r(x, y) &= \Gamma^{+\,-}(\xi)\,(y - x) \\
r(y, x) &= \Gamma^{-\,+}(\xi)\,(y - x) \\
t(x, y) &= I - \Gamma^{-\,-}(\xi)\,(y - x)
\end{aligned}
\tag{17}
$$

and the source vectors of this layer as

$$
\begin{aligned}
\Sigma^{+}(y, x) &= \Sigma^{+}(\xi)\,(y - x) \\
\Sigma^{-}(x, y) &= \Sigma^{-}(\xi)\,(y - x)
\end{aligned}
\tag{18}
$$

The matrices in equation (17) and the vectors in equation (18) can be computed numerically from the knowledge of the scattering albedo $\omega(x)$, the phase function $p(x, \mu, \mu')$, etc. It should be emphasized that these operators are only local approximations to the actual operators. It is therefore necessary that the layer thickness $(y - x)$ for which these operators will be computed be very small. An upper bound for the layer thickness can be set on the basis of physical argument that all elements of the transmission matrix be positive, and the elements of reflection matrix are also positive. The accuracy of the solution of the radiative transfer equation primarily depends upon the accuracy of these operators. Numerical results show that an acceptable accuracy in the computation of these operators can be achieved by taking the layer thickness to be one-tenth of the cosine values for the smallest angle in the quadrature.

Although equations (17) and (18) allow construction of the response operators and the source vectors of an infinitesimal layer, the task is far from being complete. In general, the medium for which one wishes to solve the radiative transfer equation is not an infinitesimal layer. If, however, one knows the procedure of juxtaposing two layers having one common boundary, then by repeated application of this procedure one can generate an arbitrary thick layer. The algebra of juxtaposing two layers can now be shown.

Using the notations of equations (17) and (18), equation (16) can be written as

$$
\begin{aligned}
u^{+}(y) &= t(y, x)\,u^{+}(x) + r(x, y)\,u^{-}(y) + \Sigma^{+}(y, x) \\
u^{-}(x) &= r(y, x)\,u^{+}(x) + t(x, y)\,u^{-}(y) + \Sigma^{-}(x, y)
\end{aligned}
\tag{19}
$$

Now an equation analogous to equation (19) can be written for a layer bounded between z and y (Figure 3).

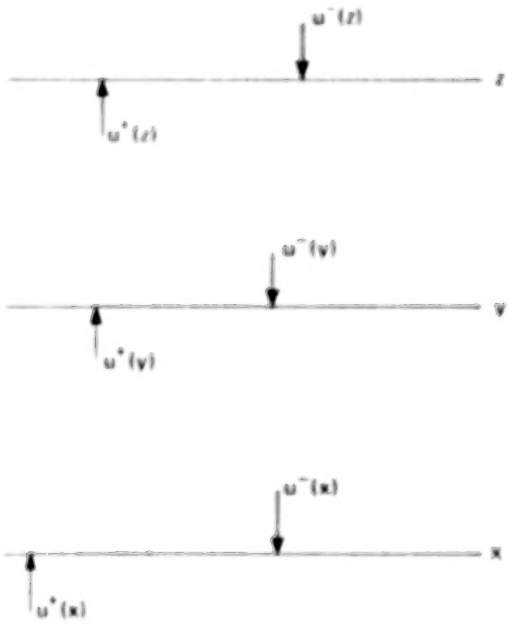

Figure 3. Radiation components between layers z and x.

$$u^+(z) = t(z, y)\, u^+(y) + r(y, z)\, u^-(z) + \Sigma^+(z, y)$$

$$u^-(y) = r(z, y)\, u^+(y) + t(y, z)\, u^-(z) + \Sigma^-(y, z) \qquad (20)$$

The boundary y being arbitrary, one can consider a layer bounded between x and z (juxtaposed layer). For this layer

$$u^+(z) = t(z, x)\, u^+(x) + r(x, z)\, u^-(z) + \Sigma^+(z, x)$$

$$u^-(x) = r(z, x)\, u^+(x) + t(x, z)\, u^-(z) + \Sigma^-(x, z) \qquad (21)$$

It is to be noted that the validity of equations (19), (20), and (21) does not depend upon layer thickness but on the principle of invariance.

The next step is to find the relationship between the operators and vectors in equation (21), and those appearing in equations (19) and (20). This relationship can be found by eliminating $u^+(y)$ and $u^-(y)$ from equations (19) and (20). By simple algebraic manipulation of equations (19) and (20), keeping in mind that these operators are matrices, one can write

$$t(z, x) = t(z, y)\,[1 - r(x, y)\, r(z, y)]^{-1}\, t(y, x)$$

$$r(x, z) = r(y, z) + t(z, y)\, r(x, y)\,[1 - r(z, y)\, r(x, y)]^{-1} r(y, x)$$

$$r(z, x) = r(y, x) + t(x, y)\, r(z, y)\,[1 - r(x, y)\, r(z, y)]^{-1}\, t(y, x) \qquad (22)$$

$$t(x, z) = t(x, y)\,[1 - r(z, y)\, r(x, y)]^{-1}\, t(y, z)$$

$$\Sigma^{+}(z, x) = t(z, y)\,[1 - r(x, y)\,r(z, y)]^{-1}\,\Sigma^{+}(y, x) + t(z, y)$$

(22 continued)

$$\cdot\,[1 - r(x, y)\,r(z, y)]^{-1}\,r(x, y)\,\Sigma^{-}(y, z) + \Sigma^{+}(z, y)$$

$$\Sigma^{-}(x, z) = t(x, y)\,[1 - r(z, y)\,r(s, y)]^{-1}\,r(z, y)\,\Sigma^{+}(y, x) + \Sigma^{-}(x, y)$$

$$+ t(x, y)\,[1 - r(z, y)\,r(x, y)]^{-1}\,\Sigma^{-}(y, z).$$

The juxtaposition relationship expressed in equation (22) is basic for layer juxtaposition, and the validity of the mathematics do not depend upon the layer thickness. If one expands the inverse of the matrices appearing in equation (22) as a series, then the exact origin of each term can be physically visualized as due to repeated reflection and transmission of radiation due to scattering. The iterative procedure of solving the radiative transfer equation accounts for such scattering by numerical iteration. In the present method, such scattering contribution has been built into the calculation. As a result, such iteration is not required.

Thus far we have outlined the procedures for constructing the response operators of an infinitesimal layer and the arbitrary thick layer. For a medium which is bounded between optical thickness $\tau = a$ and $\tau = b$, we see from equation (21) that we need to specify the intensities incident on the boundaries from outside the medium to calculate the emergent intensities. Unique emergent intensities can be obtained by imposing these boundary conditions.

The medium of interest in the present study, e.g., snow, ice, soil, and water, has different reflecting characteristics. Let R(a) and R(b) denote the Fresnel reflectivity of surface a and b. One can also assume that an intensity Y^{+} is incident on the surface a and that an intensity Y^{-} is incident on the surface b of the medium from outside (Figure 4). Then the flux conservation criteria at surface a and b can be imposed to obtain

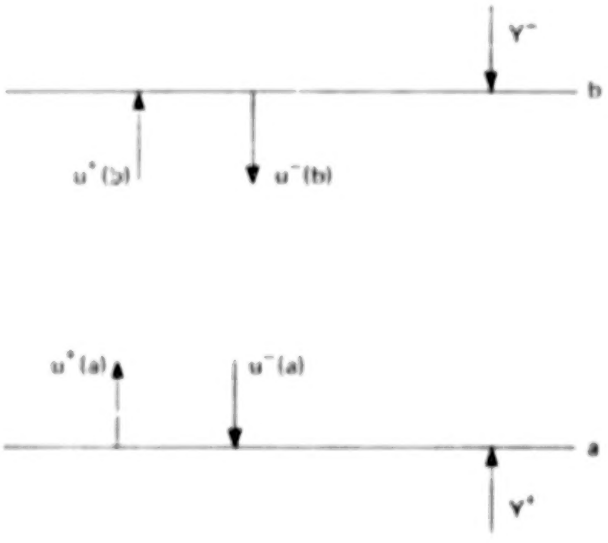

Figure 4. Reflecting characteristic intensities of Y^{+} and Y^{-} on surfaces a and b.

$$u^{+}(a) = R(a)\,u^{-}(a) + [1 - R(a)]\,Y^{+}$$

(23)

$$u^{-}(b) = R(b)\,u^{+}(a) + [1 - R(b)]\,Y^{-}$$

By substituting equation (23) into equation (21) one can solve for $u^+(b)$ and $u^-(a)$. The algebraic calculation will obtain unique solutions for the emergent intensity vector as

$$\begin{bmatrix} u^+(b) \\ u^-(a) \end{bmatrix} = \begin{bmatrix} 1 - r(a,b)\,R(b) & -t(b,a)\,R(a) \\ -t(a,b)\,R(b) & 1 - r(b,a)\,R(a) \end{bmatrix}^{-1}$$

$$\left\{ \begin{bmatrix} t(b,a) & r(a,b) \\ r(b,a) & t(a,b) \end{bmatrix} \begin{bmatrix} [1 - R(a)]\,Y^+ \\ [1 - R(b)]\,Y^- \end{bmatrix} + \begin{bmatrix} \Sigma^+(b,a) \\ \Sigma^-(a,b) \end{bmatrix} \right\} \tag{24}$$

The observable intensities are obtained from equation (24). Refer to Figure 5 for the boundary conditions of radiative transfer. Then the upwelling brightness at b and

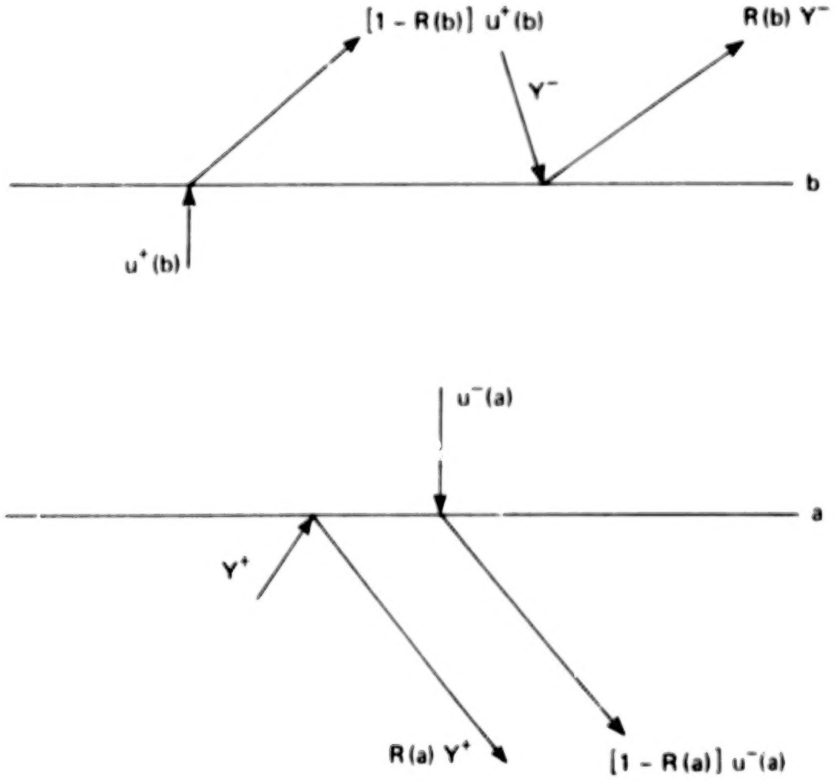

Figure 5. Boundary conditions of radiative transfer for layer a and b.

down-welling brightness at a can be expressed as:

$$T_B^+ = [1 - R(b)]\, u^+(b) + R(b)\, Y^-$$

$$T_B^- = [1 - R(a)]\, u^-(a) + R(a)\, Y^+ \qquad (25)$$

Based on the previous discussion, a computer program has been prepared (Reference 13) to solve the radiative transfer equation. The numerical accuracy of the program was tested by calculating the law of darkening for Rayleigh and isotropic scattering cases for which S. Chandrasekhar had given exact numerical results. In both cases the accuracy was found to be better than 0.1 percent. Figure 6 shows the results of Rayleigh scattering obtained using 9-point Lobatto and 7-point Gauss quadratures. Because this numerical method is non-iterative, the computer program is economically feasible for both acquisition time and storage.

We will now present the comparison of numerical results obtained by using the previous numerical method with other single particle scattering calculations (References 2 and 4). For this purpose we have used the Rayleigh phase matrix:

$$p(\tau, \mu, \mu') = \frac{3}{4} \begin{pmatrix} 2(1-\mu^2)(1-\mu'^2) + \mu^2\mu'^2 & \mu^2 \\ \mu'^2 & 1 \end{pmatrix} \qquad (26)$$

This phase matrix is valid when the radius of the particle is small compared to the wavelength of radiation. When the particle size is large one must use a Rayleigh-Debye or Mie phase matrix (Reference 14).

In A. W. England's paper (Reference 4) the microwave brightness temperature and its polarization were calculated as a function of the view angle for different cases of scattering albedo. The discrete angle method for obtaining an analytic solution (Reference 8) was used and the resulting set of coupled linear algebraic equations was solved numerically to obtain the brightness temperature. To obtain the exact solution using this method one needs to solve an infinite set of coupled equations. This had been accomplished by S. Chandrasekhar for some specific cases of scattering. Numerically, however, only a finite set of coupled equations can be solved, which leads to a truncation error (Reference 2). A quantitative estimate of this truncation error is extremely difficult to resolve. In Figure 7, we show the comparison of our calculated values with those obtained by A. W. England (Reference 4). This agreement is reassuring and does indicate that the solution obtained by A. W. England has converged to the same accuracy as the results of the present calculation, a conservative estimate of which is about 1 percent.

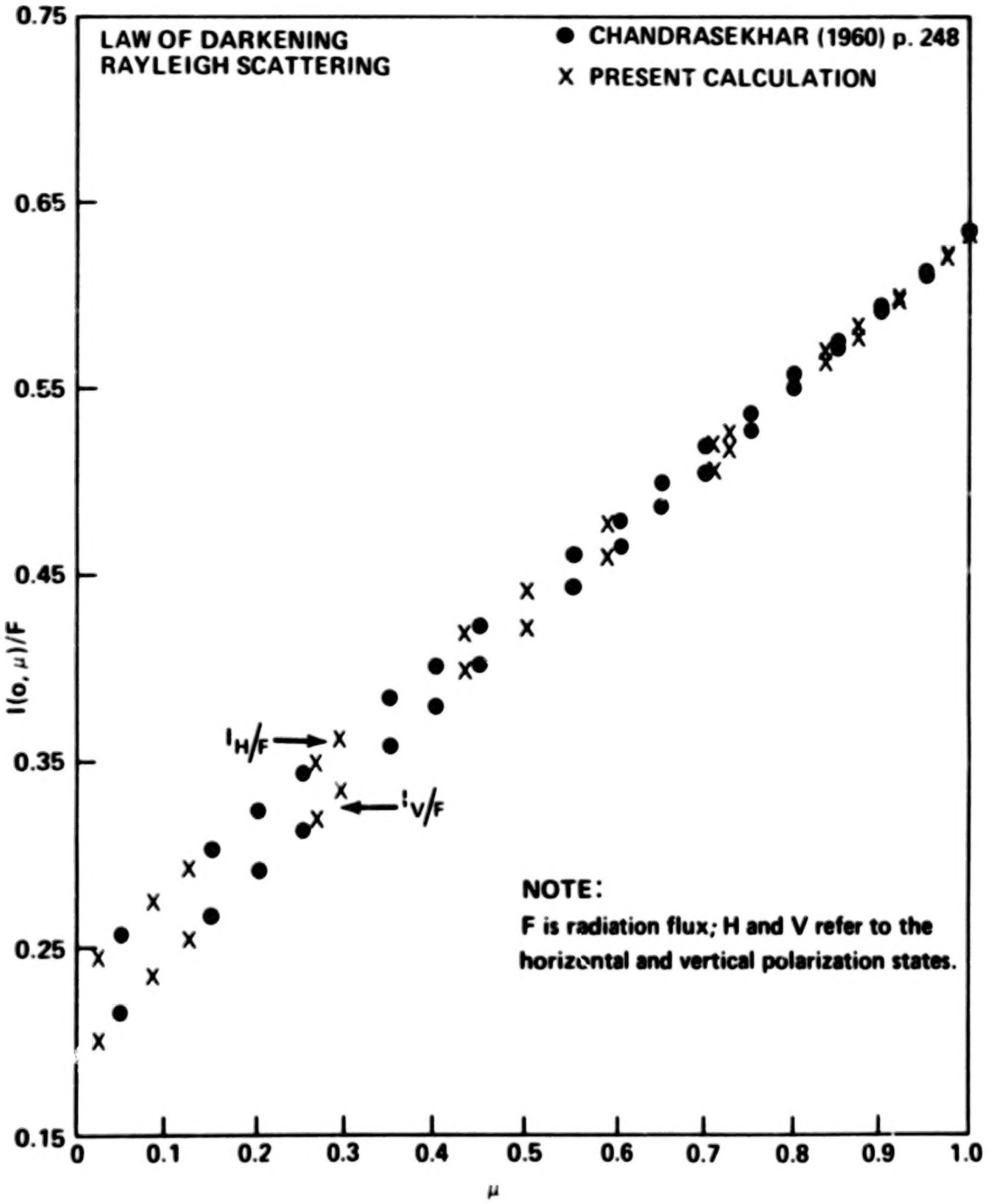

Figure 6. Results of law of darkening in Rayleigh scattering semi-infinite plane parallel atmosphere.

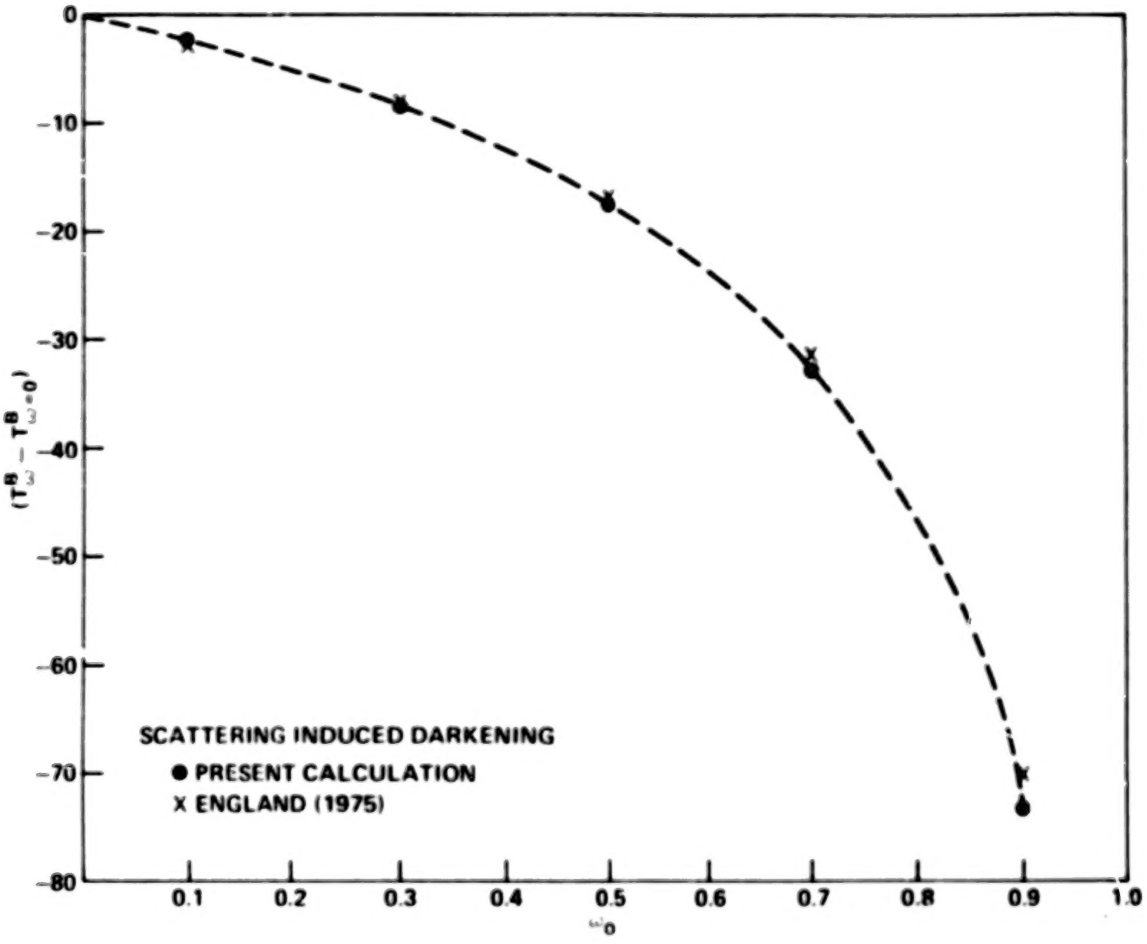

Figure 7. Results of emission darkening, comparison with A. W. England's calculations (1975).

BRIGHTNESS TEMPERATURE OF THE POLAR FIRN

The calculation of the brightness temperature of the polar firn requires the specification of a single scattering albedo $\omega(\tau)$, physical temperature within the medium $B(\tau)$, the scattering phase matrix $p(\tau, \mu, \mu')$, and the reflection coefficient at the medium boundary. In the single particle scattering approach, the albedo can be calculated from the knowledge of the scattering and the extinction coefficients of the particle. These coefficients depend upon the radius of the particle and its refractive index. For ice particles, with which we are concerned, the specification of size is sufficient to determine the scattering coefficient. The extinction coefficient of the particle on the other hand depends on the imaginary part of the index of refraction which is less sensitive to the crystal size. Calculations of T. C. Chang et al. (Reference 3) show that for ice at 273 K the extinction coefficient is about an order of magnitude higher than for ice at 253 K. Although this sensitivity can be used to distinguish temperature profiles, it also introduces some uncertainty in quantitative comparison with

remotely measured brightness temperature. It is also to be noted that the imaginary part of the index of refraction changes considerably with the presence of impurities (Reference 15). For continental shelf ice the effect of impurities may be negligible.

H. J. Zwally (Reference 7) has performed a regression study of the crystal size data for different snow depths obtained by A. J. Gow (References 5 and 6) at various locations in the South and North Polar regions. Using the Mie scattering formula (Reference 3), H. J. Zwally has provided expressions for scattering per unit length γ_s in terms of snow depth. In Table 1 we note these expressions, $\gamma_s (m^{-1})$, for which we have calculated the brightness temperature.

Table 1

Location and Mean Annual Surface Temperature and Scattering Per Unit Length (Zwally 1977)

Location	T_m* (K)	$\gamma_s (m^{-1})$
South Pole, Antarctica 90° S	222	0.222 + 0.00863 z
Byrd, Antarctica 79° 59'S 120° 01'W	245	0.152 + 0.0968 z
Camp Century, Greenland 77° 11'N 61° 10'W	249	0.163 + 0.0647 z
Inge Lehmann, Greenland 77° 57'N 39° 11'W	243	0.162 + 0.1178 z

*Mean annual surface temperature.

z is snow depth in meters.

We have mentioned that absorption per unit length is quite insensitive to the crystal size and depends largely on the imaginary part of the refractive index (n"). Although the choice of n" is not completely arbitrary, its exact value is difficult to obtain. Since the qualitative and quantitative behavior of the brightness temperature for values of n" has been studied in detail by T. C. Chang et al. (Reference 3), we have used an intermediate value, n" = 0.00055 (Reference 16) in this study. The value of the Mie absorption coefficient γ_a for this n" has been found to be $\gamma_a = 0.15$ (References 3 and 7). The single scattering albedo is defined as

$$\omega = \frac{\gamma_S}{\gamma_a + \gamma_S} \tag{27}$$

Therefore, the depth variation of ω depends on the depth variation of γ_S and γ_a.

Since γ_a varies with the physical temperature (Reference 16) of the snow, an analytic expression for depth and seasonal variation of polar snow temperature has been used (Reference 7).

$$B(z,t) = 250 - 15\,e^{-0.7z}\cos[0.99(t-84) - (97 + 20z)] \tag{28}$$

The maximum surface temperature occurs at time t = 0 and t = 365 and minimum temperature is for time t = 365/2. The mean temperature of the surface and the asymptotic temperature is 250 K and the amplitude of variation at the surface is 30 K. This mean temperature is quite acceptable for three of the locations given in Table 1. For the South Pole we have used the observed mean annual temperature of 222 K.

Calculated brightness temperature values for various locations and times are given in Table 2. The agreement between the calculated and the observed values for the North Polar region is quite good. For the South Polar region, the calculated values are slightly higher than the observed values. These results indicate that the magnitude for the scattering and absorption coefficients used are reasonable values. However, the calculated brightness temperatures are quite different from the results reported by H. J. Zwally (Reference 7). Without using the empirical parameter introduced by H. J. Zwally to adjust the scattering coefficient, our calculated brightness temperatures for all locations would be higher than those calculated by Zwally. For the South Polar region our calculated brightness temperatures are about 8 K higher than the observed values, which indicate that the values of the scattering albedo need to be increased for this study.

One source of uncertainty in the quantitative comparison discussed above was the choice of the value for n". This choice is crucial because absorption coefficient (γ_a) depends on this value. We have not incorporated in our calculation the temperature dependence of n" (Reference 16). The value of n" which we have used in our calculation (n" = 0.0005) corresponds to the temperature of ice at 253 K. To illustrate the effect of different values of n", we have studied the dependence of brightness temperature on n" by taking the scattering parameter (γ_S) of the Byrd station. The physical temperature distribution was taken for the time t = 365/4 which gives the surface temperature of 250 K. The results of our calculation are shown in Figure 8. Note that as the value of n" decreases, the absorption coefficient (γ_a) also decreases and we see the expected decrease in the brightness temperature. It is

Table 2

Comparison of Observed and Calculated Brightness Temperatures of Locations in Table 1

Location	t*	Calculated Brightness Temperature	Observation (ESMR)
South Pole, Antarctica	1	193.4	185
	365/4	191.5	180
	365/2	183.9	175
Byrd, Antarctica	1	216.3	210
	365/4	213.7	205
	365/2	204.5	200
Camp Century, Greenland	1	217.15	225
	365/4	214.9	215
	365/2	206.1	210
Inge Lehmann, Greenland	1	215.0	225
	365/4	212.2	215
	365/2	202.8	210

*t is the time parameter as shown in equation (28).

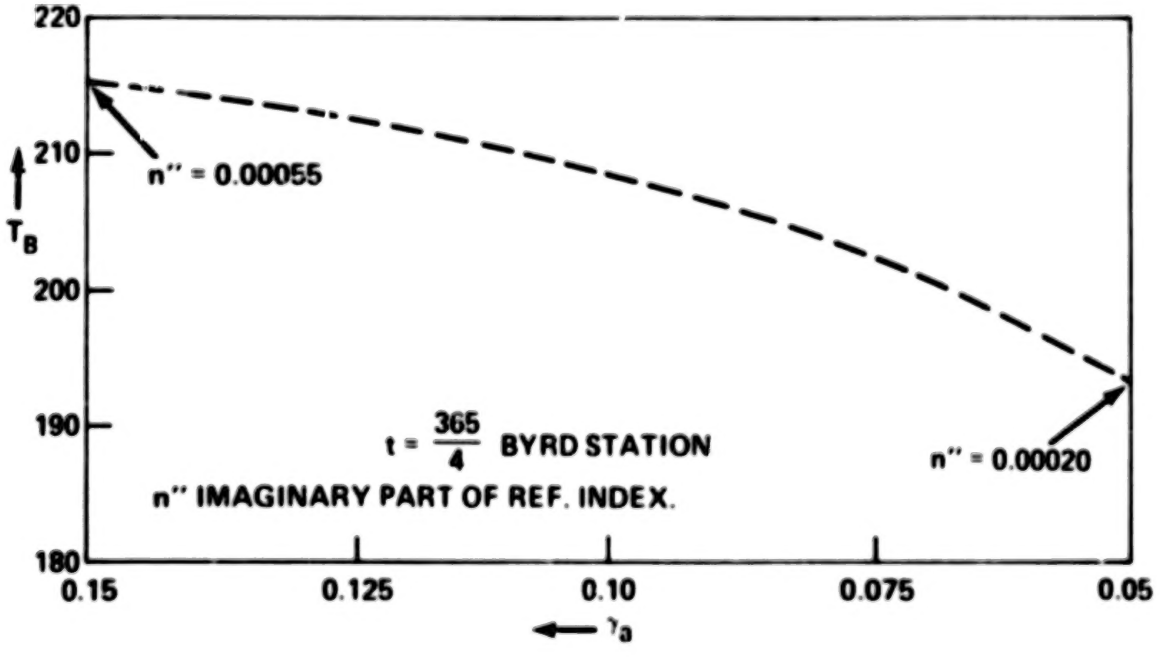

Figure 8. Dependence of brightness temperature on n'', the imaginary part of index of refraction.

interesting to note that the observed brightness temperature at the Byrd Station was approximately 210 K.

SUMMARY AND CONCLUSIONS

A microscopic single particle scattering model has been used along with measured crystal size and temperature variation with depth to provide a quantitative explanation of observed brightness temperatures of the South Polar and North Polar regions. This extends the calculations performed by T. C. Chang et al. (Reference 3) by taking into account the variations of grain size and temperature with depth. For the North Polar region, the calculated brightness temperatures are in good agreement with the observations, but for the South Polar region our calculations give higher brightness temperatures than observed. Probable cause of these discrepancies are: (1) uncertainty in the measurement of n'', (2) neglect of the dependence of n'' on temperature, and (3) neglect of snow density variation with depth.

Based on the single particle scattering model, the calculated brightness temperatures correspond to the data obtained from the Nimbus-5 ESMR experiment over Greenland and Antarctica. Using the same scattering and absorption coefficients that were used by H. J. Zwally, we find that our calculated brightness temperatures are significantly higher than those calculated by Zwally. This discrepancy is probably due to the approximate analytic solution of the radiative transfer equation used in his calculations of the brightness temperature values. In view of these findings, our calculations would provide a more realistic brightness temperature estimate for the polar firn.

Apart from the independent particle scattering model discussed above, there are alternate explanations for the source of microwave scattering and absorption for radio brightness temperatures of Antarctica and continental glaciers which have been studied by A. S. Gurvich et al. (Reference 17), A. Stogryn (Reference 18), and L. Tsang and J. A. Kong (Reference 19). In these studies, the source of microwave scattering is the fluctuation of the dielectric constant of the media (Reference 20). The brightness temperature calculated, based on these models, depends upon the variance and the correlation length of the fluctuation of the dielectric media. Physically this scattering mechanism is as plausible as scattering by independent ice grains, and it is reasonable to believe that these two scattering mechanisms co-exist in the medium and should be considered together in the quantitative calculation.

ACKNOWLEDGMENTS

The authors wish to thank P. Gloersen of the National Aeronautics and Space Administration/Goddard Space Flight Center and A. S. Milman of the Systems and Applied Sciences Corporation, for helpful suggestions and comments made during the preparation of this manuscript.

Goddard Space Flight Center
National Aeronautics and Space Administration
Greenbelt, Maryland, October 1977

REFERENCES

1. Gloersen, P., T. T. Wilheit, T. C. Chang, W. Nordberg, and W. J. Campbell, "Microwave Maps of the Polar Ice of the Earth," *Bull. Am. Meteor. Soc.*, **55**, pp. 1442-1448, 1974.

2. England, A. W., "Thermal Microwave Emission From a Half-space Containing Scatterers," *Radio Sci.*, **9**, pp. 447-454, 1974.

3. Chang, T. C., P. Gloersen, T. Schmugge, T. T. Wilheit, and H. J. Zwally, "Microwave Emission From Snow and Glacier Ice," *J. of Glaciology*, **16**, pp. 23-39, 1976.

4. England, A. W., "Thermal Microwave Emission From Scattering Layer," *J. Geophys. Res.*, **80**, pp. 4484-4496, 1975.

5. Gow, A. J., "On The Rate of Growth of Grains and Crystals in South Polar Firn," *J. of Glaciology*, **8**, 241-52, 1969.

6. Gow, A. J., *"Depth-time-temperature Relationship of Ice Crystal Growth in Polar Region,"* U. S. Army Cold Region Research and Engineering Laboratory, Research Report 300, 1971.

7. Zwally, H. J., "Microwave Emission and Accumulation Rate of Polar Firn," *J. of Glaciology*, **18**, pp. 195-215, 1977.

8. Chandrasekhar, S., *"Radiative Transfer,"* Dover Publication, New York, pp. 161-182, 1960.

9. Bellman, R. E., R. E. Kalaba, and M. C. Prestrud, *"Invariant Imbedding and Radiative Transfer in Slabs of Finite Thickness,"* American Elsevier Publication, New York, pp. 5-35, 1963.

10. Redheffer, R., "On the Relation of Transmission-line Theory to Scattering and Transfer," *J. of Math. Phys.*, **41**, pp. 1-41, 1962.

11. Preisendorfer, R. W., *"Radiative Transfer in Discrete Spaces,"* Pergamon Press, Oxford, England, 1965.

12. Grant, I. P., and G. E. Hunt, "Discrete Space Theory of Radiative Transfer," *Proc. Roy. Soc. (London)*, **313**, pp. 199-216, 1969.

13. Choudhury, B. J., *"Method of Invariant Imbedding and Radiative Transfer in an Inhomogenious Medium,"* Computer Sciences Corporation, System Sciences Division, Technical Memo., CSC-TM/6122, 1977.

14. Van de Hulst, H., *"Light Scattering by Small Particles,"* John Wiley and Sons, Inc., New York, 1957.

15. Hoekstra, P., and P. Cappillino, "Dielectric Properties of Sea and Sodium Chloride Ice at UHF and Microwave Frequencies," *J. of Geophys. Res.*, **76**, pp. 4922-31, 1971.

16. Cumming, W. A., "The Dielectric Properties of Ice and Snow at 3.2 Centimeters," *J. of Appl. Physics*, **23**, pp. 768-73, 1952

17. Gurvich, A. S., V. I. Kalinin, and D. T. Matveyen, "Influence of the Internal Structure of Glaciers on Their Thermal Radio Emission," *J. Atmos. and Oceanic Phys.*, **9**, pp. 1247-1256, 1973.

18. Stogryn, A., "Electromagnetic Scattering by Random Dielectric Constant Fluctuations in a Bounded Medium," *Radio Sci.*, **9**, pp. 509-18, 1974.

19. Tsang, L., and J. A. Kong, "Thermal Microwave Emission From Half-space Random Medium," *Radio Sci.*, **11**, pp. 599-609, 1976.

20. Tatarskii, V. I., *"Wave Propagation in a Turbulent Medium,"* translated from Russian by R. Silverman, McGraw Hill Publication, New York, pp. 59-70, 1961.

1. Report No. NASA TP-1212	2. Government Accession No.	3. Recipient's Catalog No.
4. Title and Subtitle Microwave Emission From Polar Firn		5. Report Date April 1978 6. Performing Organization Code 910
7. Author(s) A. T. C. Chang and B. J. Choudhury		8. Performing Organization Report No.
9. Performing Organization Name and Address Goddard Space Flight Center Greenbelt, Maryland 20771		10. Work Unit No. 11. Contract or Grant No. 13. Type of Report and Period Covered Technical Paper
12. Sponsoring Agency Name and Address National Aeronautics and Space Administration Washington, D.C. 20546		14. Sponsoring Agency Code

15. Supplementary Notes

16. Abstract

The microwave emission from a half-space medium characterized by coordinate dependent scattering and absorbing centers has been calculated by numerically solving the radiative transfer equation by the method of invariant imbedding. Rayleigh scattering phase functions and scattering induced polarization of the radiation have been included in the calculation. For uniform temperature distribution within the medium, the results of A. T. C. Chang and B. J. Choudhury calculations agree well with those by A. W. England. Using the scattering and extinction data of polar firn as compiled by H. J. Zwally, the brightness temperature has been calculated for the 1.55 cm wavelength. For the North Polar region, the results of our calculations are in agreement with the Nimbus-5 scanning radiometer experiment. This study is the first quantitative comparison of the results of numerical calculation using the actual measured information of crystal size with the observed data.

17. Key Words (Selected by Author(s))	18. Distribution Statement
Rayleigh scattering phase functions, Polar firn	Unclassified – Unlimited Cat. 46

19. Security Classif. (of this report)	20. Security Classif. (of this page)	21. No. of Pages	22. Price*
Unclassified	Unclassified	22	$4.00

* For sale by the National Technical Information Service, Springfield, Virginia 22161

NASA-Langley, 1978